Mon. Not. R. Astron. Soc. **265,** 513–523 (1993)

Resonance-line polarization in a moving medium: solution in the comoving frame with complete frequency redistribution

S. Sengupta
Indian Institute of Astrophysics, Bangalore 560 034, India

Accepted 1993 May 11. Received 1993 April 19

ABSTRACT

We study the effect of differential radial velocity on the distribution of line intensities and line polarization along the line of sight of an extended stellar atmosphere stratified in parallel planes. The main purpose of this paper is to understand the behaviour of line polarization in an extended and expanding atmosphere. The atmospheric models could represent the photospheric layers of early-type stars. We consider, for simplicity, complete redistribution of frequency. The velocities of expansion of the medium are set at 5, 20 and 50 mean thermal units with two different velocity laws. The results are compared with that of the static case. It is found that large effects are generated in the polarized radiation field when differential radial expansion is taken into account.

Key words: line: formation – polarization – radiative transfer – stars: atmospheres.

1 INTRODUCTION

In the absence of any external magnetic field, the absorption of an anisotropic radiation field by an atom leads to a non-uniform population of the Zeeman sublevels of the excited state and the coherences among such levels. As a consequence, the re-emitted radiation field is linearly polarized. Such a two-level atomic model is a quantum analogue of the Rayleigh scattering of the continuum radiation.

The basic theory of resonance-line polarization and its diagnostic potential in solar observations have been studied extensively by Stenflo and co-workers (Stenflo 1976; Stenflo & Stenholm 1976; Stenflo, Baur & Elmore 1980). Detailed theoretical discussions can also be found in Mitchell & Zemanski (1934), Hamilton (1947) and Landi degl'Innocenti (1984). The direct solution in plane-parallel geometry (pp) has been presented by Rees & Saliba (1982, and references therein).

All these authors employed radiative transfer in a static medium. We study in this paper the same problem but for a medium having a differential velocity gradient. It is well known from observations that early-type stars, giant and supergiant stars, symbiotic stars and luminous late-type stars possess differential velocities in the radial direction in their outer layers, with speeds ranging from 2 to 100 mean thermal units (mtu). These stars show degrees of polarization ranging from 0.1 to 5 per cent in the optical band (Coyne et al. 1988). It is therefore very important to study the effect of velocity on line polarization.

In our study we consider the radiative transfer equation in the comoving frame (Castor 1972) with the plane-parallel approximation. Scalar line formation in the comoving frame for both plane-parallel and spherically symmetric cases has been well studied by Mihalas and co-workers (Mihalas et al. 1976a; Mihalas, Kunasz & Hummer 1976b) and Peraiah (1980a, b). The advantages in working in the comoving frame have been discussed in detail by Mihalas (1978).

In this paper we use the Peraiah method (Peraiah 1984) for solving the plane-parallel radiative transfer problem in the comoving frame, and present a large number of results. For the sake of simplicity we assume the complete frequency distribution (CRD) approximation.

In the next section we present the relevant equations. In Section 3 we discuss the method of obtaining solutions and the boundary conditions. The atmospheric parameters are given in Table 1. In Section 4 we discuss the results and draw specific conclusions. Finally, we summarize the general features of our investigation in Section 5.

2 THE TRANSFER EQUATIONS

In general, a linearly polarized beam is represented by the three Stokes parameters $\boldsymbol{I}$, $\boldsymbol{Q}$ and $\boldsymbol{U}$. In a plane-parallel medium, because of the axial symmetry of the radiation field, only two parameters are required to define the polarization state of the radiation field (Chandrasekhar 1960): $\boldsymbol{I}$, the specific intensity of the radiation field, and $\boldsymbol{Q}$ ($=I_l - I_r$, where I_l and I_r are the components that are perpendicular

Table 1. Atmospheric model parameters.

Model	τ	ϵ	β	B
1...	10^5	10^{-3}	3×10^{-5}	1
2...	10^6	10^{-4}	5×10^{-6}	1
3...	10^6	10^{-6}	5×10^{-6}	1
4...	10^4	10^{-6}	5×10^{-4}	1
5...	10^4	0	0	1
6...	10^5	0	0	1
7...	10^6	0	0	1

and parallel to the surface, respectively), the polarized intensity. The degree of linear polarization $p = \boldsymbol{Q}/\boldsymbol{I}$ gives the measure of the anisotropy of the diffuse radiation field. We have adopted a sign convention such that a positive value of p corresponds to polarization directed perpendicular to the surface.

The transfer equation for polarized radiation is a vector analogue of the non-LTE two-level atom line transfer equation in the comoving frame (Mihalas et al. 1976a; see also Peraiah 1984). The equation of transfer for plane-parallel symmetry in the comoving frame is given by

$$\mu\frac{\partial}{\partial z}\begin{bmatrix}I_l(x,\mu,z)\\ I_r(x,\mu,z)\end{bmatrix}=k_L[\beta+\phi(x)]\left\{\begin{bmatrix}S_l(x,\mu,z)\\ S_r(x,\mu,z)\end{bmatrix}-\begin{bmatrix}I_l(x,\mu,z)\\ I_r(x,\mu,z)\end{bmatrix}\right\}+\left[\mu^2\frac{dv(z)}{dz}\right]\frac{\partial}{\partial x}\begin{bmatrix}I_l(x,\mu,z)\\ I_r(x,\mu,z)\end{bmatrix}, \quad (1)$$

where $\mu=\cos\theta(\mu\in[0,1])$ and θ is the angle between the Stokes specific intensity vector and the axis of symmetry z; $x=(\nu-\nu_0)/\Delta\nu_D$, where ν is the frequency in Hz, ν_0 is the line centre frequency and $\Delta\nu_D$ is the Doppler width, which is assumed to be constant throughout the atmosphere. The quantity β is the ratio k_c/k_L of the opacity due to continuous absorption per unit interval x to that in the line (k_L is the frequency-integrated line opacity). The normalized absorption profile is represented by a Voigt function

$$\phi(x)=H(a,x)/\sqrt{\pi}\,, \quad (2)$$

where a represents a constant ratio of the damping width to the Doppler width. The total source vector is given by

$$\mathbf{S}(x,\mu,z)=\begin{bmatrix}S_l(x,\mu,z)\\ S_r(x,\mu,z)\end{bmatrix}=\frac{\phi(x)\mathbf{S}^L(x,\mu,z)+\beta\mathbf{S}^c(z)}{\beta+\phi(x)}. \quad (3)$$

$\mathbf{S}^L$ and $\mathbf{S}^c$ refer to the source vectors in the line and continuum respectively, where

$$\mathbf{S}^c(z)=0.5B(z)\mathbf{1},\ \mathbf{1}=(1,1)^T. \quad (4)$$

The line source vector is given by

$$\mathbf{S}^L(x,\mu,z)=\frac{(1-\varepsilon)}{\phi(x)}\int_{-\infty}^{\infty}dx'\int_{-1}^{+1}\mathbf{R}(x,\mu,x',\mu')\times\begin{bmatrix}I_l(x',\mu',z)\\ I_r(x',\mu',z)\end{bmatrix}d\mu'+\frac{\varepsilon}{2}B(z)\mathbf{1}, \quad (5)$$

where ε is the probability per scattering that a photon is destroyed by collisional de-excitation. The redistribution matrix $\mathbf{R}(x,\mu,x',\mu')$ is defined according to a hybrid model prescription by Rees & Saliba (1982), and is given by

$$\mathbf{R}(x,\mu,x',\mu')=\mathbf{P}(\mu,\mu')R(x,x'), \quad (6)$$

which retains the angular correlation in the phase function $\mathbf{P}(\mu,\mu')$ essential for scattering polarization and mimics the frequency correlation via the angle-averaged scalar redistribution function $R(x,x')$ for isotropic scattering.

The phase matrix for resonance scattering is given by Chandrasekhar (1960) as

$$\mathbf{P}(\mu,\mu')=\frac{3}{8}E_1\begin{bmatrix}2(1-\mu^2)(1-\mu'^2)+\mu^2\mu'^2 & \mu^2\\ \mu'^2 & 1\end{bmatrix}+\frac{(1-E_1)}{4}\begin{bmatrix}1 & 1\\ 1 & 1\end{bmatrix}. \quad (7)$$

To maximize the polarization we assume a $J=0\rightarrow1$ transition so that E_1 and $\mathbf{P}(\mu,\mu')$ take the form of the well-known Rayleigh phase matrix. For the sake of simplicity we have considered the complete redistribution function given by

$$R(x,x')=\phi(x)\phi(x'). \quad (8)$$

Equation (1) can now be rewritten as

$$\mu\frac{\partial}{\partial z}\begin{bmatrix}I_l(x,\mu,z)\\ I_r(x,\mu,z)\end{bmatrix}=\phi(x)k_L\mathbf{S}^L(x,\mu,z)+k_c\mathbf{S}^c(z)-[\phi(x)k_L+k_C]\begin{bmatrix}I_l(x,\mu,z)\\ I_r(x,\mu,z)\end{bmatrix}+\mu^2\frac{dv(z)}{dz}\frac{\partial}{\partial x}\begin{bmatrix}I_l(x,\mu,z)\\ I_r(x,\mu,z)\end{bmatrix}, \quad (9)$$

and for the oppositely directed beam

$$-\mu\frac{\partial}{\partial z}\begin{bmatrix}I_l(x,-\mu,z)\\ I_r(x,-\mu,z)\end{bmatrix}=\phi(x)k_L\mathbf{S}^L(x,-\mu,z)+k_c\mathbf{S}^c(z)-[\phi(x)k_L+k_C]\begin{bmatrix}I_l(x,-\mu,z)\\ I_r(x,-\mu,z)\end{bmatrix}+\mu^2\frac{dv(z)}{dz}\frac{\partial}{\partial x}\begin{bmatrix}I_l(x,-\mu,z)\\ I_r(x,-\mu,z)\end{bmatrix}, \quad (10)$$

where $\mathbf{S}^{L}$ and $\mathbf{S}^{c}$ are given by equations (5) and (4) respectively.

We must emphasize here that all the quantities mentioned above are to be understood to be measured in the comoving frame of the fluid.

3 METHOD

3.1 Method of computation

We have employed the Peraiah method (Peraiah 1980a,b, 1984) for solving the plane-parallel radiative transfer problem in the comoving frame. Our main purpose is to develop the reflection and transmission operators that embody all the physical information contained in the present problem. The medium under consideration is divided into a number of layers. The transmission, reflection and source vectors are computed for all the layers. For a thick layer, the so-called star product, which is essentially a doubling algorithm, is used.

To start with, we discretize equations (9) and (10). For frequency discretization, we choose discrete frequency points x_i and weights a_i so that

$$\int_{-\infty}^{\infty} \phi(x)\, f(x) \approx \sum_{i=-I}^{+I} a_i f(x_i), \qquad \sum_{i=-I}^{+I} a_i = 1,$$

and for angular discretization we choose angular points μ_j and weights c_j such that

$$\int_0^1 f(\mu)\, \mathrm{d}\mu \approx \sum_{j=1}^{m} b_j f(\mu_j), \qquad \sum_{j=1}^{m} b_j = 1.$$

We integrate the equation over an interval $[Z_n, Z_{n+1}]\times[\mu_{j-1/2}, \mu_{j+1/2}]$ defined on a two-dimensional grid. By choosing the roots μ_j and the weights c_j of the Gauss–Legendre quadrature formula of order J over (0, 1), we calculate the sets $\mu_{j+1/2}$ and $\mu_{j-1/2}$ as given by

$$\mu_{j+1/2} = \sum_{k=1}^{j} c_k$$

and

$$\mu_{j-1/2} = \sum_{k=1}^{j-1} c_k; \qquad j = 1, 2, 3 \ldots J.$$

We define the boundary of the angular interval as $\mu_{1/2} = 0$.

Integrating equations (9) and (10), first in the interval $[\mu_{j-1/2}, \mu_{j+1/2}]$ and then over the spatial cell $[Z_n, Z_{n+1}]$, we obtain

$$\begin{aligned}
&\mathbf{M}_{2J}[\mathbf{I}^{+}_{i,n+1} - \mathbf{I}^{+}_{i,n}] + \tau_{n+1/2}[\beta \mathbf{I}_{2J} + \boldsymbol{\phi}^{+}_{i}]_{n+1/2} \mathbf{I}^{+}_{i,n+1/2} \\
&\quad = \tau_{n+1/2}[\rho\beta \mathbf{I}_{2J} + \varepsilon \boldsymbol{\phi}^{+}_{i}]_{n+1/2} B_{n+1/2} \mathbf{h}_{2J} + \frac{1}{2}\tau_{n+1/2}(1-\varepsilon) \\
&\quad \times \sum_{i'=-I}^{+I} [a^{++}_{i',n+1/2}\, \mathbf{R}^{++}_{i,i',n+1/2} \mathbf{c}_{2J} \mathbf{I}^{+}_{i',n+1/2} \\
&\quad + a^{+-}_{i',n+1/2} \mathbf{R}^{+-}_{i,i',n+1/2} \mathbf{c}_{2J} \mathbf{I}^{-}_{i',n+1/2}] + \mathbf{M}'_{2J} \mathbf{d} \mathbf{I}^{+}_{i',n+1/2} \Delta v_{n+1/2}
\end{aligned} \tag{11}$$

and

$$\begin{aligned}
&-\mathbf{M}_{2J}[\mathbf{I}^{-}_{i,n+1} - \mathbf{I}^{-}_{i,n}] + \tau_{n+1/2}[\beta \mathbf{I}_{2J} + \boldsymbol{\phi}^{+}_{i}]_{n+1/2} \mathbf{I}^{-}_{i,n+1/2} \\
&\quad = \tau_{n+1/2}[\rho\beta \mathbf{I}_{2J} + \varepsilon \boldsymbol{\phi}^{+}_{i}]_{n+1/2} B_{n+1/2} \mathbf{h}_{2J} \\
&\quad + \frac{1}{2}\tau_{n+1/2}(1-\varepsilon) \sum_{i'=-I}^{+I} [a^{-+}_{i',n+1/2} \mathbf{R}^{-+}_{i,i',n+1/2} \\
&\quad \mathbf{c}_{2J} \mathbf{I}^{+}_{i',n+1/2} + a^{--}_{i',n+1/2} \mathbf{R}^{--}_{i,i',n+1/2} \mathbf{c}_{2J} \mathbf{I}^{-}_{i',n+1/2}] \\
&\quad + \mathbf{M}'_{2J} \mathbf{d} \mathbf{I}^{-}_{i',n+1/2} \Delta v_{n+1/2}\,.
\end{aligned} \tag{12}$$

Here the subscripts n, $n+1$, $n+1/2$ refer to quantities at Z_n, Z_{n+1}, $Z_{n+1/2}$, where $n+1/2$ refers to a suitable average over the cell, i.e.

$$Z_{n+1/2} = \frac{1}{2}(Z_{n+1} + Z_n), \qquad \Delta Z_{n+1/2} = Z_{n+1} - Z_n,$$

$$\tau_{n+1/2} = k_{\mathrm{L}}(Z_{n+1/2}) \Delta Z_{n+1/2},$$

$$\mathbf{I}^{+}_{i,n+1/2} = \frac{1}{2}(\mathbf{I}^{+}_{i,n+1} + \mathbf{I}^{+}_{i,n}),$$

$$\mathbf{I}^{-}_{i,n+1/2} = \frac{1}{2}(\mathbf{I}^{-}_{i,n+1} + \mathbf{I}^{-}_{i,n}).$$

The redistribution matrices are

$$\mathbf{R}^{++}_{i,i'}(z) = \begin{bmatrix} \mathbf{R}^{++}_{i,i',n}(1,1)\, \mathbf{R}^{++}_{i,i',n}(1,2) \\ \mathbf{R}^{++}_{i,i',n}(2,1)\, \mathbf{R}^{++}_{i,i',n}(2,2) \end{bmatrix},$$

where the block matrices corresponding to the phase matrix are defined as

$$\mathbf{R}^{++}_{i,i',n}(\alpha,\beta) = \begin{bmatrix} \mathbf{R}^{++}_{i,1,i',1,n}(\alpha,\beta) & \ldots & \mathbf{R}^{++}_{i,1,i',J,n}(\alpha,\beta) \\ & \vdots & \\ \mathbf{R}^{++}_{i,J,i',1,n}(\alpha,\beta) & \ldots & \mathbf{R}^{++}_{i,J,i',J,n}(\alpha,\beta) \end{bmatrix},$$

$$\mathbf{R}^{++}_{i,j,i',j',n} = \mathbf{R}(x_i \mu_j; x'_i \mu'_j; z_n),$$

$$\mathbf{M}_{2J} = \begin{bmatrix} \mathbf{M}_J & \mathbf{0} \\ \mathbf{0} & \mathbf{M}_J \end{bmatrix}; \qquad \mathbf{M}_J = [\mu_j \delta_{jj'}],$$

$$\mathbf{C}_{2J} = \begin{bmatrix} \mathbf{C}_J & \mathbf{0} \\ \mathbf{0} & \mathbf{C}_J \end{bmatrix}; \qquad \mathbf{C}_J = [c_j \delta_{jj'}],$$

$$\mathbf{I}^{+}_{i}(z) = [\mathbf{I}^{+}_{i,n}(l) \ldots \mathbf{I}^{+}_{i,n}(r)]^{\mathrm{T}},$$

$$\mathbf{I}^{-}_{i}(z) = [\mathbf{I}^{-}_{i,n}(l) \ldots \mathbf{I}^{-}_{i,n}(r)]^{\mathrm{T}},$$

$$\mathbf{I}^{+}_{i,n}(l) = [\mathbf{I}_{i,1,n}(l), \ldots \mathbf{I}_{i,J,n}(l)]^{\mathrm{T}},$$

$$\mathbf{I}^{-}_{i,n}(l) = [\mathbf{I}_{i,-1,n}(l), \ldots \mathbf{I}_{i,-J,n}(l)]^{\mathrm{T}}$$

[$\mathbf{I}^{+}_{i,n}(r)$ and $\mathbf{I}^{-}_{i,n}(r)$ are defined similarly],

$$\boldsymbol{\phi}^{\pm}_{i}(z) = \begin{bmatrix} \boldsymbol{\phi}^{\pm}_{i,n}(l) & \mathbf{0} \\ \mathbf{0} & \boldsymbol{\phi}^{\pm}_{i,n}(r) \end{bmatrix},$$

$$\boldsymbol{\phi}^{\pm}_{i,n}(l) = [\phi_{i\pm j,n}(l)\, \delta_{jj'}],$$

$$\boldsymbol{\phi}^{\pm}_{i,n}(r) = [\phi_{i\pm j,n}(r)\, \delta_{jj'}]$$

(where j, $j' = 1, 2, 3, \ldots J$, and δ_{jk} is a Dirac delta function), and

$$\mathbf{h}_{2J} = [\mathbf{1}_J \mathbf{1}_J]^{\mathrm{T}}; \qquad \mathbf{1}_J = [1, 1, 1, \ldots 1]^{\mathrm{T}}.$$

The comoving terms given in equations (9) and (10) are represented by the term $\mathbf{M}'_{2J}\,\mathbf{d}I^{\pm}_{i',n+1/2}\Delta V_{n+1/2}$, where

$$\mathbf{M}'_{2J} = \begin{bmatrix} \mathbf{M}'_J & \mathbf{0} \\ \mathbf{0} & \mathbf{M}'_J \end{bmatrix}, \qquad \mathbf{M}'_J = [\mu_j^2 \delta_{jj'}],$$

$$\Delta V_{n+1/2} = V_{n+1} - V_n,$$

$$\mathbf{d} = \begin{bmatrix} \mathbf{d}' & 0 \\ 0 & \mathbf{d}' \end{bmatrix},$$

where the matrix $\mathbf{d}'$ is determined from the condition of flux conservation, where

$$d'_i = (x_{i+1} - x_{i-1})^{-1} \text{ for } i = 1, 2, 3, \ldots I-1 \text{ and } d'_1 = d'_I = 0.$$

Dropping the indices J and I (which represent the numbers of angle and frequency points respectively) we can now rewrite equations (11) and (12) as

$$\mathbf{M}[\mathbf{I}^+_{n+1} - \mathbf{I}^+_n] + \tau_{n+1/2}\boldsymbol{\Phi}^+_{n=1/2}\mathbf{I}^+_{n+1/2} = \tau_{n+1/2}\mathbf{S}^+_{n+1/2}$$
$$+\frac{1}{2}(1-\varepsilon)\tau_{n+1/2}[\mathbf{R}^{++}\mathbf{W}^{++}\mathbf{I}^+ + \mathbf{R}^{+-}\mathbf{W}^{+-}\mathbf{I}^-]_{n+1/2}$$
$$+\mathbf{M}'\mathbf{d}\mathbf{I}^+_{n+1/2}\Delta V_{n+1/2} \qquad (13)$$

and

$$\mathbf{M}[\mathbf{I}^-_n - \mathbf{I}^+_{n+1}] + \tau_{n+1/2}\boldsymbol{\Phi}^-_{n=1/2}\mathbf{I}^-_{n+1/2} = \tau_{n+1/2}\mathbf{S}^-_{n+1/2}$$
$$+\frac{1}{2}(1-\varepsilon)\tau_{n+1/2}[\mathbf{R}^{-+}\mathbf{W}^{-+}\mathbf{I}^+ + \mathbf{R}^{--}\mathbf{W}^{--}\mathbf{I}^-]_{n+1/2}$$
$$+\mathbf{M}'\mathbf{d}\mathbf{I}^-_{n+1/2}\Delta V_{n+1/2} \qquad (14)$$

$$\mathbf{M} = [\mu\delta_{kk'}], \qquad \mathbf{I}^{\pm}_n = [I^{\pm}_{k,n}], \qquad \mathbf{M}' = [\mu^2\delta kk'],$$
$$I^{\pm}_{k,n} = I(x_i, \pm\mu_j; z_n; p),$$

where

$$k = j + (i-1)J + (p-1)IJ; \qquad 1 \le k \le pIJ,$$

p being the polarization state number (in our case $p = 2$),

$$\boldsymbol{\Phi}^{\pm}_{n+1/2} = (\beta + \phi^{\pm}_k)_{n+1/2}\delta_{kk'}; \qquad \phi^{\pm}_{k,n+1/2} = \phi(x_i, \pm\mu_j, z_{n+1/2}; p),$$

and

$$\mathbf{S}^{\pm}_{n+1/2} = [\rho\beta + \varepsilon\phi^{\pm}_k]_{n+1/2}B_{n+1/2}\delta_{kk'}.$$

$\mathbf{W}^{++}_{n+1/2}$ are the weights matrices defined as $\mathbf{W}^{++}_{n+1/2} = [W^{++}_{k,n+1/2}\delta_{kk'}]$, with $\phi^+_{k,n+1/2}W^{++}_{k,n+1/2} = a^{++}_{i,n+1/2}c_j$ (ρ is an unspecified parameter).

The renormalized weights of integration are defined by

$$a^{++}_{i,n+1/2} = \frac{a_i\phi_{k,n+1/2}}{\sum_{k=1}^{2IJ} a_i\, c_j \sum_{k'=1}^{2IJ} R^{++}_{k,k',n+1/2}}.$$

The average intensities $I^{\pm}_{n+1/2}$ are approximated by the diamond scheme (Grant 1986) given by

$$(\mathbf{1} - \mathbf{X}_{n+1/2})\mathbf{I}^+_n + \mathbf{X}_{n+1/2}\mathbf{I}^+_{n+1} = \mathbf{I}^+_{n+1/2}, \qquad (15a)$$
$$(\mathbf{1} - \mathbf{X}_{n+1/2})\mathbf{I}^-_{n+1} + \mathbf{X}_{n+1/2}\mathbf{I}^-_n = \mathbf{I}^-_{n+1/2}, \qquad (15b)$$

with

$$\mathbf{X}_{n+1/2} = \frac{1}{2}\begin{bmatrix} \mathbf{X}' & \mathbf{0} \\ \mathbf{0} & \mathbf{X}' \end{bmatrix}; \qquad \mathbf{X}' = \frac{1}{2}\mathbf{1}; \qquad \mathbf{1} = \begin{bmatrix} \mathbf{1} & \mathbf{0} \\ \mathbf{0} & \mathbf{1} \end{bmatrix},$$

$\mathbf{1}$ being the unit matrix.

Introducing equations (15a) and (15b) into equations (13) and (14), we write the resulting equations in the form of the interaction principle (Grant & Hunt 1969a,b) (see Appendix A) and, comparing these with the interaction principle, we obtain the 'cell' reflection and transmission matrices and source vectors. These are listed in Appendix B.

In the plane-parallel case the method is unconditionally stable and provides accurate solutions as long as the conventional normalization conditions are satisfied.

The frequency-independent l and r components of the source function along a particular angle have been determined in the comoving frame, and using these source functions the line profiles and the polarization profiles seen by an observer at infinity can now be determined.

3.2 Boundary conditions

We solve the problem for two kinds of boundary conditions: (1) the radiation incident on either side of the atmosphere, and (2) the frequency derivative $\partial\mathbf{I}/\partial x$ appearing in the comoving term. In the first case, we assume that there is no incident radiation on either side of the atmosphere (except in a few cases), i.e. $\mathbf{I}(x, \mu) = 0 (\tau = 0, \mu = 0, \tau = T, \mu > 0)$. In the second case we assume that in the continuum $\partial\mathbf{I}/\partial x = 0$.

4 RESULTS AND DISCUSSION

It is well known that resonance polarization is governed by collisional rates, by the geometry of the medium in which the lines are formed, which affects the anisotropy of the radiation field, and by non-LTE mechanisms, such as frequency redistribution. The collisional rates are sensitive to the distribution of matter inside the medium. Except for the geometry of the medium, all the other processes are greatly affected by the inclusion of a radial velocity field. The velocity field is associated with the temperature of the stellar atmosphere.

We have employed two types of velocity rule, guided by Mihalas et al. (1976b):

$$V(n) = V_A + \frac{V_B - V_A}{N} \times n$$

and

$$V(n) = V_A + cV_B[\tan^{-1}(an + b) - \tan^{-1}(a + b)].$$

Here V_A is the velocity at the innermost layer, which is always kept equal to 0, and V_B is that at the outermost layer, i.e. the terminal velocity. We have taken $V_B = 5$, 20, 50 mean thermal units (mtu) and have also included the static case for a comparative study. N is the total number of layers, which is

generally taken to be 50 to 100, n is the layer number, and a, b and c are constants.

In the first case the velocity increases linearly, and in the second case the velocity increases rapidly from the innermost layer, the gradient then becoming steeper until it finally reaches its maximum value.

We have calculated the total intensity profile along the line of sight as well as the percentage of the degree of polarization. In all figures the ratio of the flux at a particular frequency to that in the continuum is shown.

Figs 1(a), 3(a) and 5(a) represent the line profile in a purely scattering medium with the linear velocity rule. In the static case the line profile is symmetric, whereas in the non-static case the profiles are Doppler-shifted towards the blue region, resembling p-Cygni profiles. The emergent flux at the line of sight decreases as the velocity increases. This is similar to the isotropic case.

Figs 2(a), 4(a) and 6(a) represent the line profile in a purely scattering medium with the tangential velocity rule. The sharp peaks obtained with the linear velocity rule are not seen here.

In a purely scattering static medium the polarized profile is frequency-independent, as seen in Figs 1(b)–6(b). This is purely the effect of complete frequency redistribution, and has been reported by some previous authors (Nagendra 1986). This situation is altered by the inclusion of velocity, which changes the energy of the line photons.

The degree of polarization is positive for zero, small and moderately large velocities, but negative for a large velocity in a purely scattering medium. For all types of purely scattering media the degree of polarization in a static medium is less than that in a non-static medium. This is mainly due to the blueshift in the frequency of the incident photons.

The degree of polarization takes a larger value when the velocity of the medium is small, i.e. 5 mtu, than when the velocity is moderately large, i.e. 20 mtu. This may be due to the effect of velocity on the distribution of matter. With a small velocity a large amount of matter is accumulated at

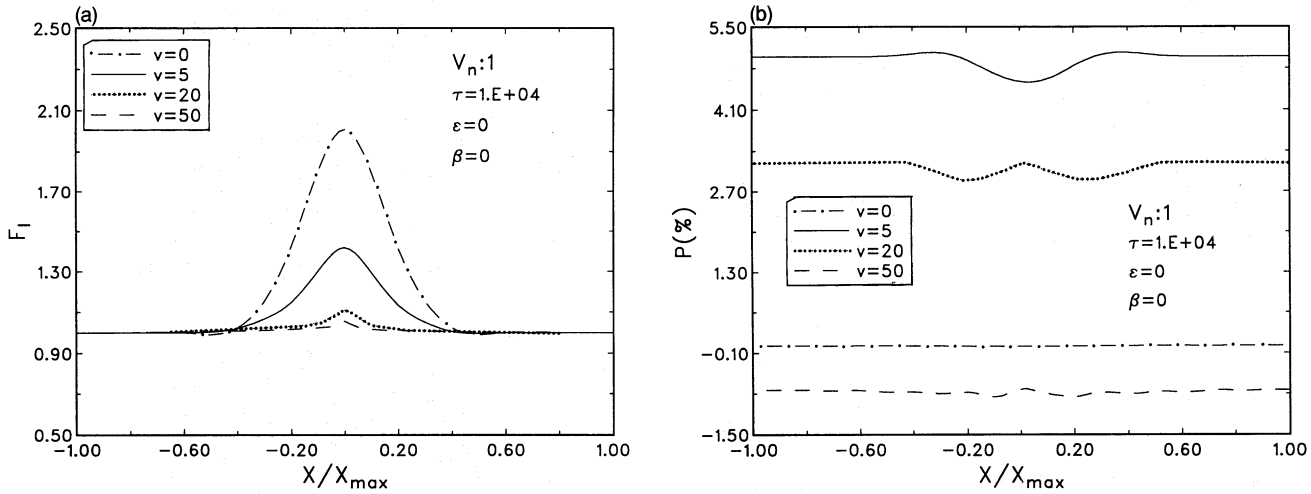

Figure 1. (a) The total flux profile along the line of sight with a linear velocity gradient (V_n: 1). In this and all subsequent figures, 'v' denotes the terminal velocity. (b) The corresponding percentage of the degree of polarization.

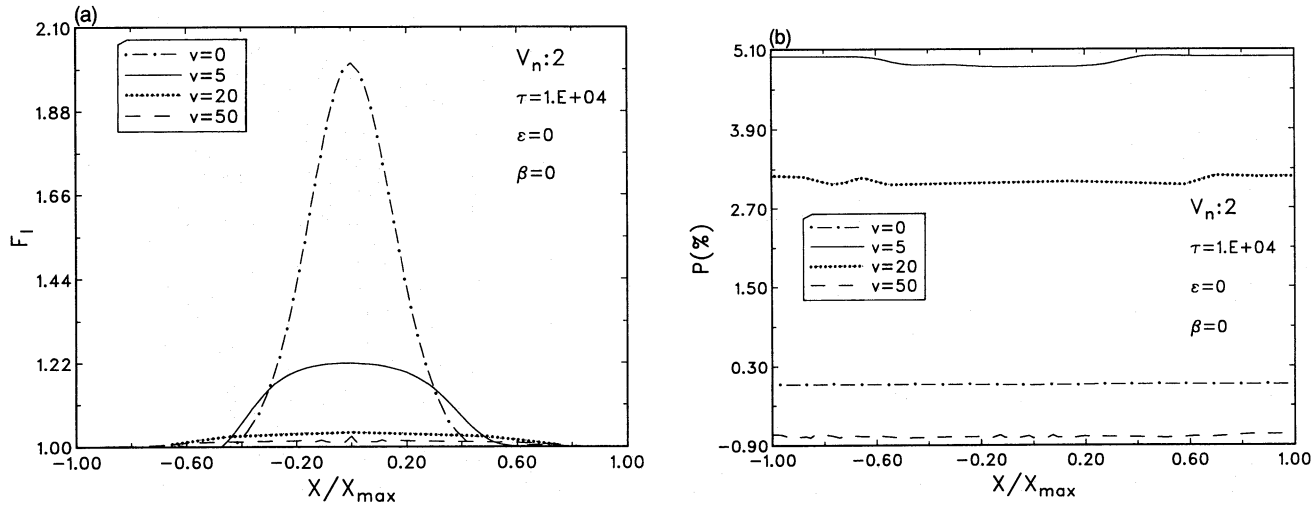

Figure 2. (a) The total flux profile along the line of sight with a tangential velocity gradient (V_n: 2). (b) The corresponding percentage of the degree of polarization.

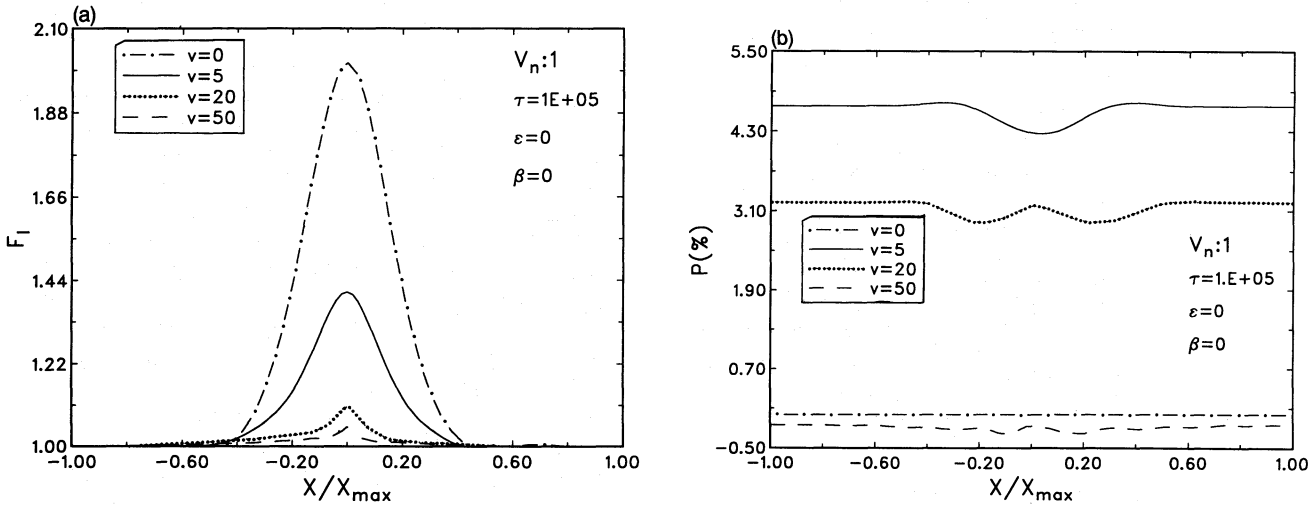

Figure 3. (a) As Fig. 1(a), but for different optical depth. (b) As Fig. 1(b), but for different optical depth.

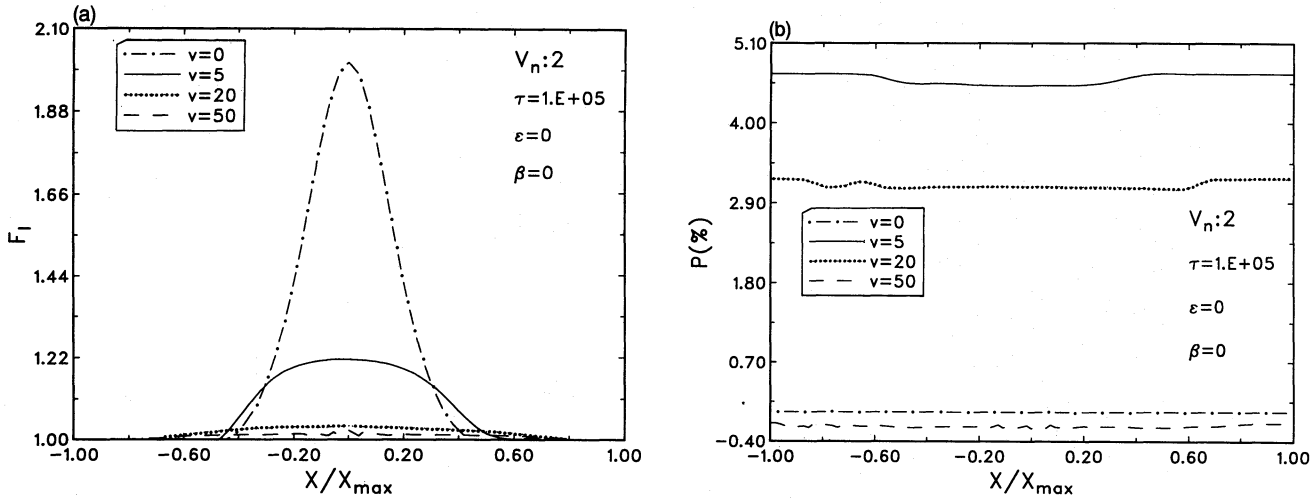

Figure 4. (a) As Fig. 2(a), but for different optical depth. (b) As Fig. 2(b), but for different optical depth.

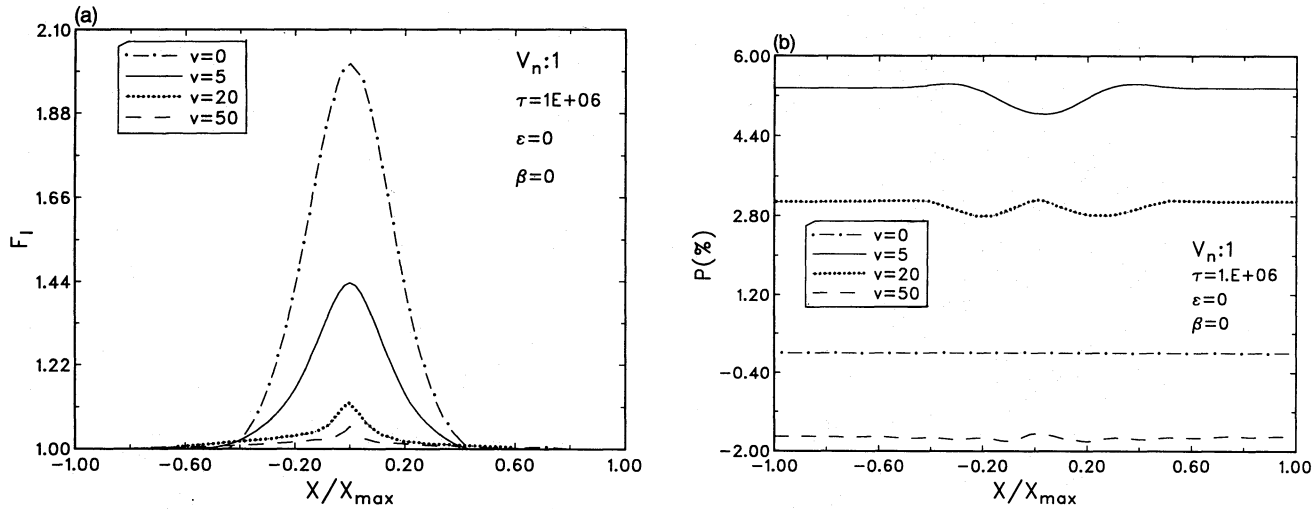

Figure 5. (a) As Fig. 1(a), but for different optical depth. (b) As Fig. 1(b), but for different optical depth.

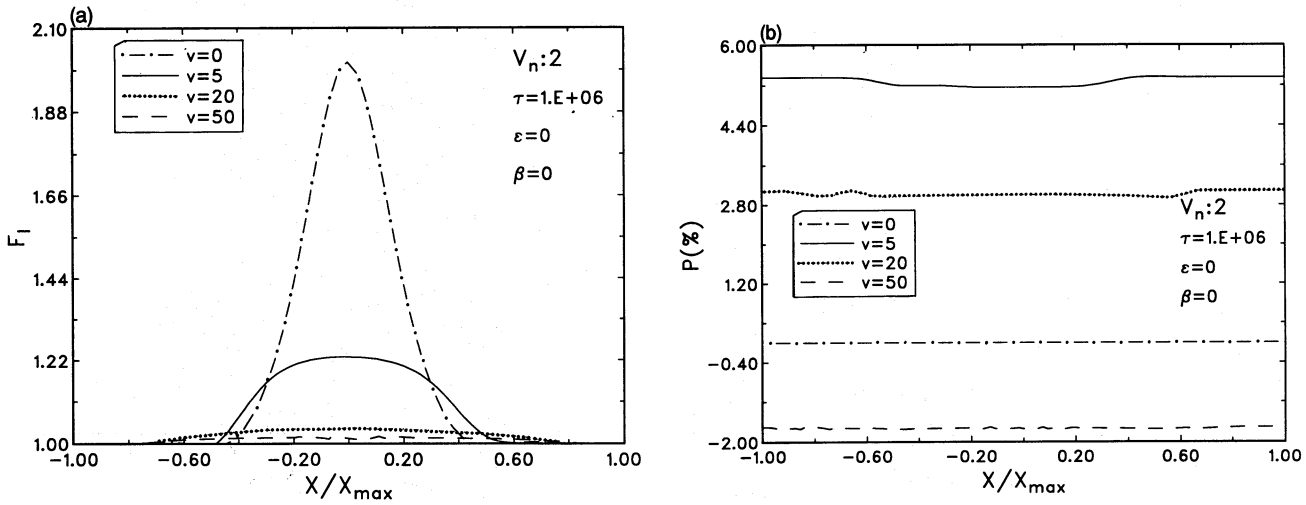

Figure 6. (a) As Fig. 2(a), but for different optical depth. (b) As Fig. 2(b), but for different optical depth.

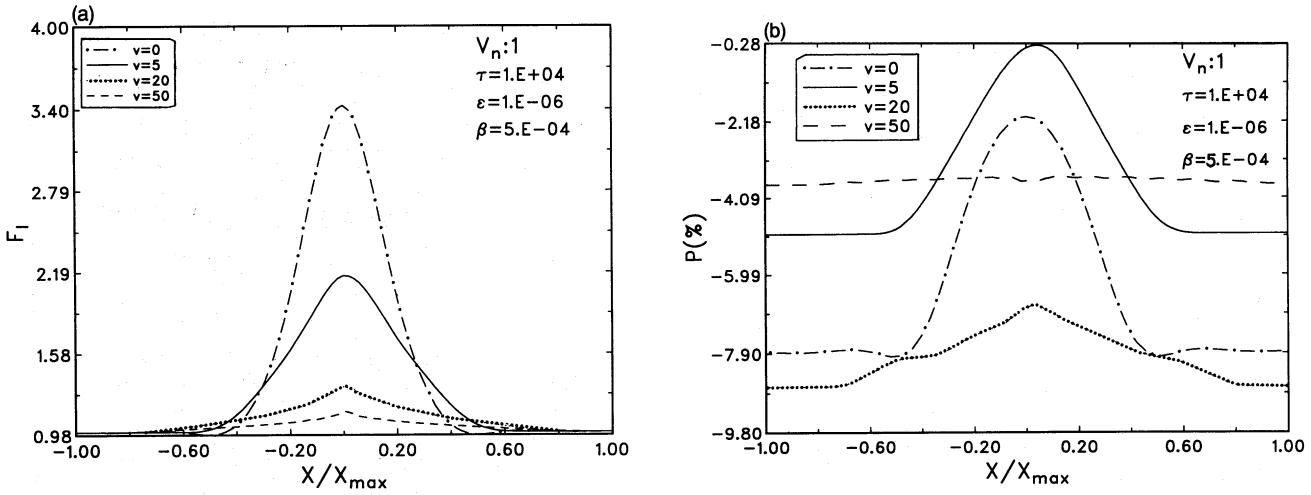

Figure 7. (a) As Fig. 1(a), but for different ε and β. (b) As Fig. 1(b), but for different ε and β.

certain positions to give rise to larger amounts of polarization. The effect of depolarization may also play an important role in this context.

For a very large velocity, e.g. 50 mtu, the incident photons become highly energetic. Also, almost all the matter is driven out towards the outer region. These give rise to a nearly frequency-independent polarized profile. This effect is seen in all the models.

We notice that with the increase in optical depth the degree of polarization increases because of the increase in the number of scatterers. Due to the adopted boundary conditions the degree of polarization is almost the same at the wings for all cases in a purely scattering medium.

The inclusion of a non-zero thermalization parameter ε changes the polarized profile significantly from that of a purely scattering medium. The line intensity is higher in this case. Unlike the case for a purely scattering medium, the degree of polarization is always negative in a medium with a non-zero thermalization parameter.

As can be seen in Figs 7(b)–14(b), the degree of polarization in a medium with a small velocity is less than in a static medium, whereas it is much higher in a medium with a moderately large velocity (20 mtu). A comparison with the purely scattering medium implies that the effect of a non-zero thermalization parameter is much greater than the effect of matter distribution, which in turn is governed by the velocity field because the velocity dilutes the medium.

With the linear velocity rule there is a sharp peak at the line centre in the polarized profile, whereas no such peak is obtained in a medium with the tangential velocity rule.

As mentioned earlier, the degree of polarization is negative and frequency-independent in a medium with a very large velocity. The degree of polarization is, however, much larger than that of a purely scattering medium. With a large velocity the degree of polarization is always a minimum at the wing, but near the line centre it is greater than the degree of polarization of a static medium as well as that of a medium having a small radial velocity. Further, we notice that the

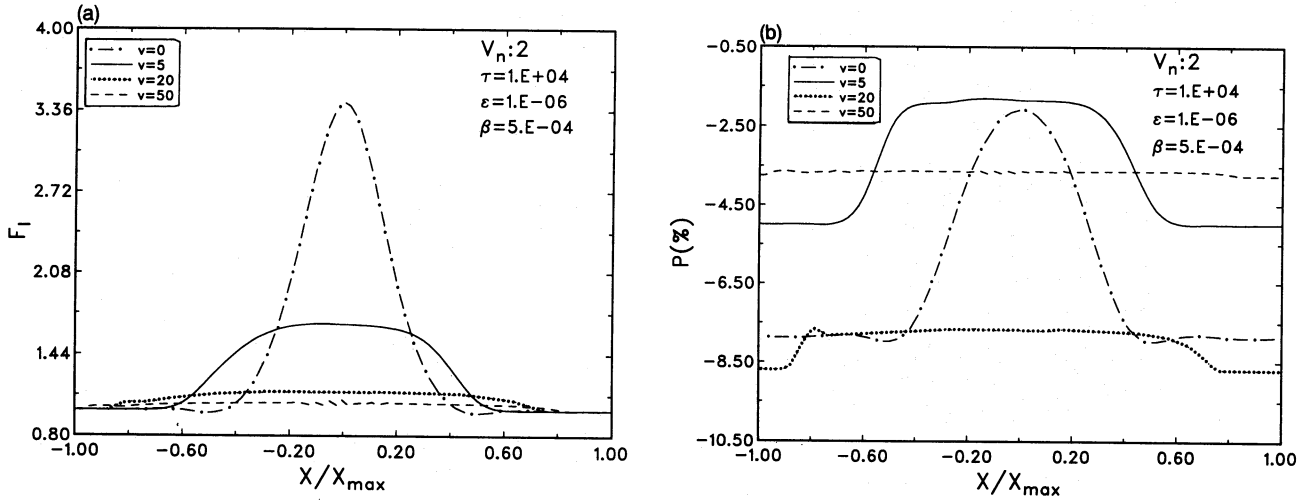

Figure 8. (a) As Fig. 2(a), but for different ε and β. (b) As Fig. 2(b), but for different ε and β.

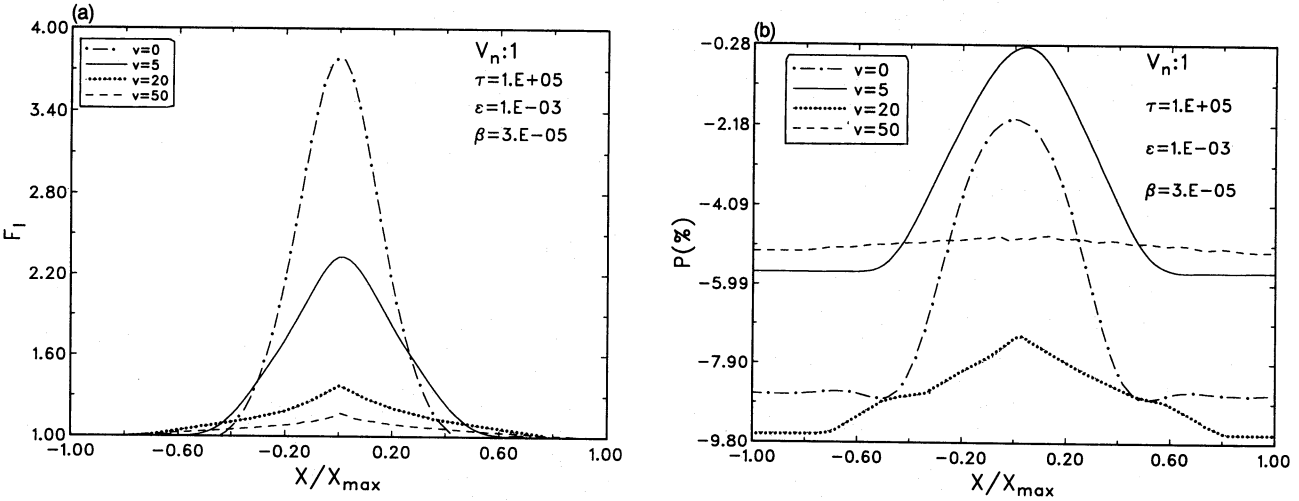

Figure 9. (a) As Fig. 1(a), but for different optical depth, ε and β. (b) As Fig. 1(b), but for different optical depth, ε and β.

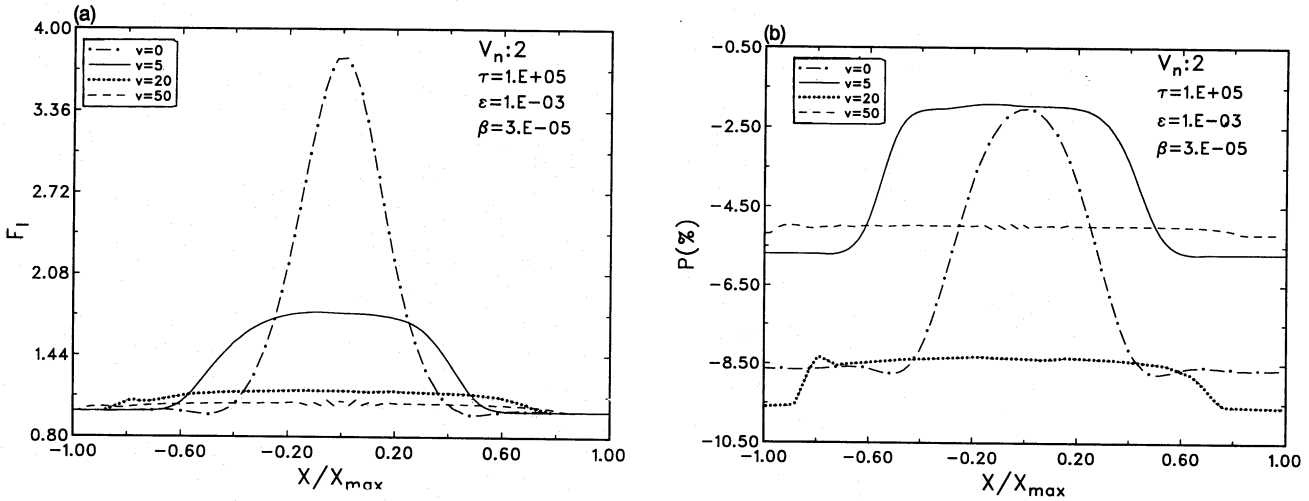

Figure 10. (a) As Fig. 2(a), but for different optical depth, ε and β (b) As Fig. 2(b), but for different optical depth, ε and β.

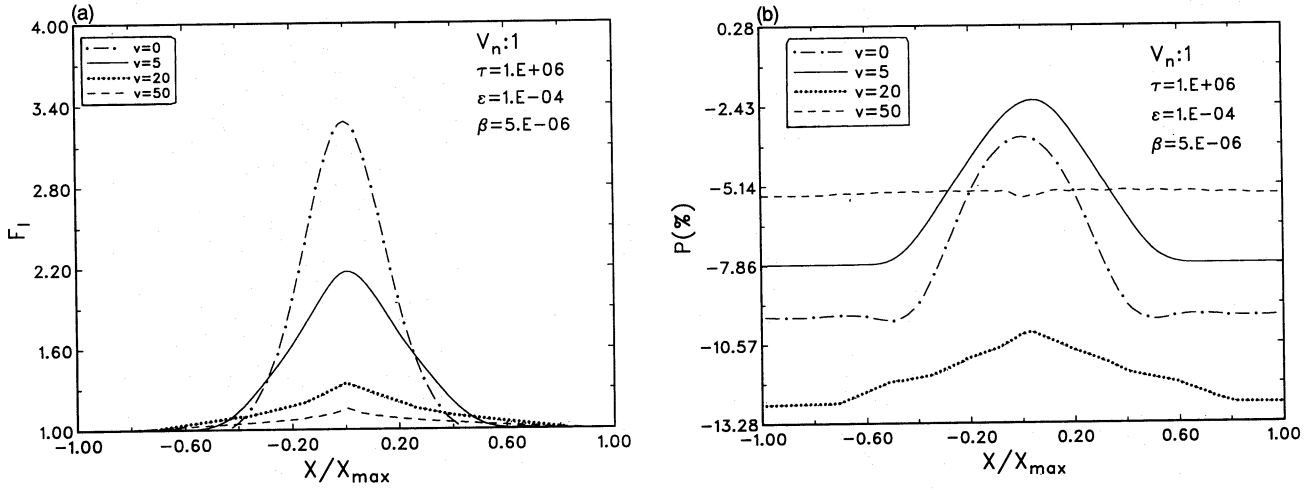

Figure 11. (a) As Fig. 1(a), but for different optical depth, ε and β. (b) As Fig. 1(b), but for different optical depth, ε and β.

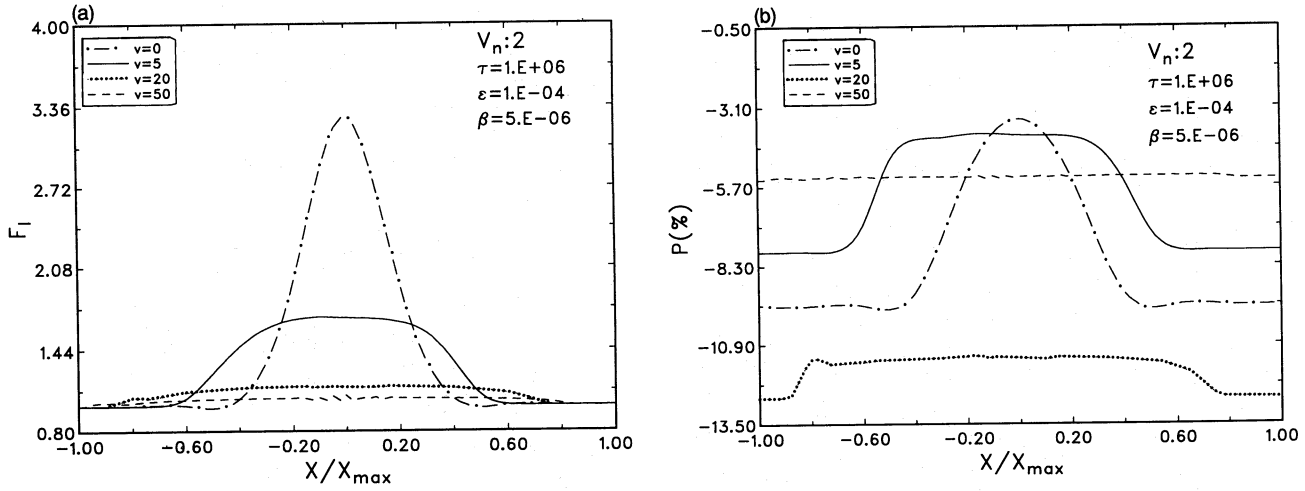

Figure 12. (a) As Fig. 2(a), but for different optical depth, ε and β. (b) As Fig. 2(b), but for different optical depth, ε and β.

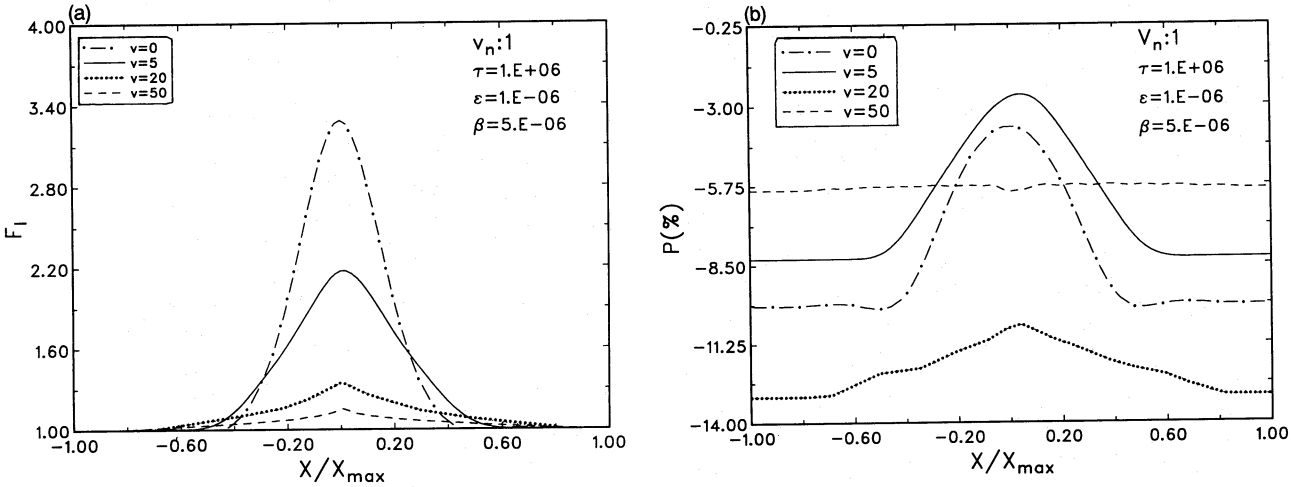

Figure 13. (a) As Fig. 1(a), but for different optical depth, ε and β. (b) As Fig. 1(b), but for different optical depth, ε and β.

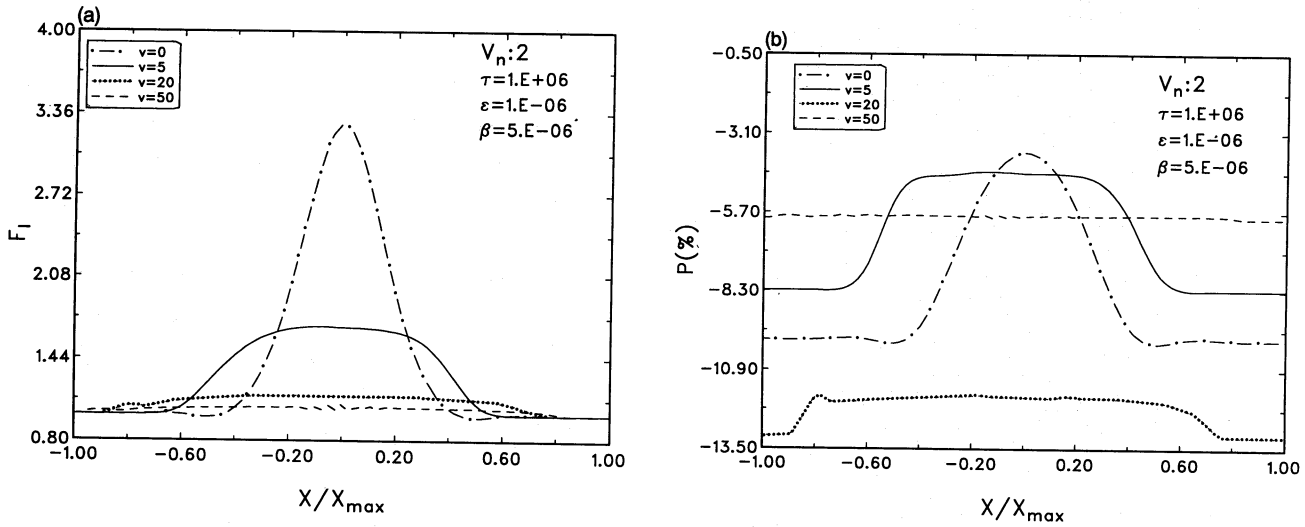

Figure 14. (a) As Fig. 2(a), but for different optical depth, ε and β. (b) As Fig. 2(b), but for different optical depth, ε and β.

polarization profile in a medium with the tangential velocity rule is nearly frequency-independent near the line centre but increases rapidly at the nearer wing. This rapid increase in polarization is also evident with the linear velocity rule. This result is due to the specific boundary conditions. It is worth mentioning that in all cases the degree of polarization increases significantly as optical depth increases.

In all the models discussed above, a complete frequency redistribution function has been adopted. In general, the partial redistribution line profiles behave like the CRD profile in the line core. One should therefore expect significant changes in the continuum with the use of a PRD function. Further, we have considered a plane-parallel geometry. For early-type stars the curvature effect will play a dominant role, since the atmosphere is very large, and so a spherically symmetric geometry is more relevant in this case. The inclusion of these two cases will, however, make the problem very complicated, as the stability and the uniqueness of the solutions will become highly conditional.

Since with different velocity gradients different effects dominate, a complete interpretation of the numerical results is non-trivial and difficult. Although the models employed here are highly idealized, they provide a reasonably good understanding of the basic features of the polarized line formation problem in a radially expanding stellar atmosphere.

The method discussed in Section 3.1 can handle the problems that arise from the coupling of the comoving points across the line profile and the local velocity gradients. The solution is calculated on the basis of the discrete space theory, which depends on the interaction principle that connects the physical properties of the medium with its transmitting and reflecting characteristics. The stability of the solution is achieved by controlling the step-size in the discretization in radial, angle and frequency integrations. The step-size is coupled to the physical conditions of the medium. The critical step-size is derived so that the transmission and the reflection functions estimated in a given shell or layer are always positive and satisfy the conservation principles. In the present calculation we find that each shell (the entire atmosphere is divided into 50 shells) is represented by several mtu of velocity. Choosing a reasonable step-size, we find a stable solution. We have used the internal field algorithm to estimate the diffuse radiation field. Thus the stability and the uniqueness are maintained. The flux is conserved up to nine decimal places.

5 CONCLUSIONS

We have presented some basic aspects of the resonance-line polarization in a radially expanding medium. We have adopted simple physical and atmospheric models for this purpose, our aim being to understand the two-level atom line polarization transfer in a plane-parallel geometry with a differential velocity gradient. We have employed the comoving frame calculation with complete frequency redistribution. It has been found that the inclusion of a velocity field substantially affects the polarization in the resonance line, and that the degree of polarization is always negative and nearly frequency-independent when a large velocity gradient is included. In a purely scattering medium the degree of polarization is maximum for a small velocity, but in a partially scattering medium it is maximum for a moderately large velocity gradient. In all cases the profiles have been obtained along the line of sight. The computations are preliminary in nature and will be useful for obtaining a general idea about the resonance-line polarization in a radially expanding plane-parallel stellar atmosphere.

ACKNOWLEDGMENTS

The author gratefully acknowledges the valuable guidance of Professor A. Peraiah in all aspects of this work. This work is financially supported by the Council for Scientific and Industrial Research, New Delhi, under its SRF scheme.

REFERENCES

Castor J. I., 1972, ApJ, 178, 779
Chandrasekhar S., 1960, Radiative Transfer. Dover, New York
Coyne G. V. S. J., Moffat A. F. J., Tapia S., Magalhaes A. M., Schulte-Ladbeck R. E., Wickramasinghe D. T. (eds), 1988, Polarized Radiation of Circumstellar Origin. Vatican Observatory, Vatican City State
Grant I. P., 1968, J. Comput. Phys., 2, 381
Grant I. P., Hunt G. E., 1969a, Proc. R. Soc. Lond. A, 313, 183
Grant I. P., Hunt G. E., 1969b, Proc. R. Soc. Lond. A, 313, 199
Hamilton D. R., 1947, ApJ, 105, 424
Landi degl'Innocenti E., 1984, Solar Phys., 91, 1
Mihalas D., 1978, Stellar Atmospheres. Freeman, San Francisco
Mihalas D., Shine R. A., Kunasz P. B., Hummer D. G., 1976a, ApJ, 205, 492
Mihalas D., Kunasz P. B., Hummer D. G., 1976b, ApJ, 206, 515
Mitchell A. C., Zemanski M. W., 1934, Resonance Radiation and Excited Atoms. Cambridge Univ. Press, Cambridge
Nagendra K. N., 1986, PhD thesis, Bangalore University
Peraiah A., 1980a, Acta Astron., 30, 525
Peraiah A., 1980b, JA&A, 1, 3
Peraiah A., 1984, in Kalkofen W., ed., Methods in Radiative Transfer. Cambridge Univ. Press, Cambridge
Rees D., Saliba G., 1982, A&A, 115, 1
Stenflo J. O., 1976, A&A, 46, 61
Stenflo J. O., Stenholm L., 1976, A&A, 46, 69
Stenflo J. O., Bauer T. G., Elmore D. F., 1980, A&A, 84, 60

APPENDIX A

Equations (13) and (14) can be written in canonical form as

$$\begin{bmatrix} \mathbf{M}+\frac{1}{2}\tau[\Phi^{+}-(\sigma/2)\mathbf{R}^{++}\mathbf{W}^{++}]-\frac{1}{2}\mathbf{M}'\mathbf{d}\Delta V & [(\tau\sigma)/4]\mathbf{R}^{+-}\mathbf{W}^{+-} \\ -[(\tau\sigma)/4]\mathbf{R}^{-+}\mathbf{W}^{-+} & \mathbf{M}+(\tau/2)[\Phi^{-}-(\sigma/2)\mathbf{R}^{--}\mathbf{W}^{--}]-\frac{1}{2}\mathbf{M}'\mathbf{d}\Delta V \end{bmatrix} \begin{bmatrix} \mathbf{I}^{+}_{n+1} \\ \mathbf{I}^{-}_{n} \end{bmatrix} =$$

$$\begin{bmatrix} \mathbf{M}+\frac{1}{2}\tau[\Phi^{+}-(\sigma/2)\mathbf{R}^{++}\mathbf{W}^{++}]-\frac{1}{2}\mathbf{M}'\mathbf{d}\Delta V & [(\tau\sigma)/4]\mathbf{R}^{+-}\mathbf{W}^{+-} \\ -[(\tau\sigma)/4]\mathbf{R}^{-+}\mathbf{W}^{-+} & \mathbf{M}+(\tau/2)[\Phi^{-}-(\sigma/2)\mathbf{R}^{--}\mathbf{W}^{--}]-\frac{1}{2}\mathbf{M}'\mathbf{d}\Delta V \end{bmatrix} \begin{bmatrix} \mathbf{I}^{+}_{n} \\ \mathbf{I}^{-}_{n+1} \end{bmatrix} + \tau \begin{bmatrix} \mathbf{S}^{+} \\ \mathbf{S}^{-} \end{bmatrix},$$

where $\sigma=(1-\varepsilon)$ and the subscript $(n+1/2)$ is left out for convenience.

APPENDIX B

We define the following auxiliary quantities:

$$\mathbf{G}^{+-}=[\mathbf{I}-\mathbf{g}^{+-}\mathbf{g}^{-+}]^{-1},$$

$$\mathbf{G}^{-+}=[\mathbf{I}-\mathbf{g}^{-+}\mathbf{g}^{-+}]^{-1},$$

$$\mathbf{g}^{+-}=\frac{\tau}{2}\Delta^{+}\mathbf{Y}_{-},$$

$$\mathbf{g}^{-+}=\frac{\tau}{2}\Delta^{-}\mathbf{Y}_{+},$$

$$\mathbf{D}=\mathbf{M}-\frac{\tau}{2}\mathbf{Z}_{-},$$

$$\mathbf{A}=\mathbf{M}-\frac{\tau}{2}\mathbf{Z}_{+},$$

$$\Delta^{+}=\left[\mathbf{M}+\frac{\tau}{2}\mathbf{Z}_{+}\right]^{-1},$$

$$\Delta^{-}=\left[\mathbf{M}+\frac{\tau}{2}\mathbf{Z}_{-}\right]^{-1},$$

$$\mathbf{Z}_{+}=\Phi^{+}-\frac{\sigma}{2}\mathbf{R}^{++}\mathbf{W}^{++}-\frac{1}{2}\mathbf{M}'\mathbf{d}\Delta V,$$

$$\mathbf{Z}_{-}=\Phi^{-}-\frac{\sigma}{2}\mathbf{R}^{--}\mathbf{W}^{--}-\frac{1}{2}\mathbf{M}'\mathbf{d}\Delta V,$$

$$\mathbf{Y}_{+}=\frac{\sigma}{2}\mathbf{R}^{-+}\mathbf{W}^{-+},$$

$$\mathbf{Y}_{-}=\frac{\sigma}{2}\mathbf{R}^{+-}\mathbf{W}^{+-}.$$

The transmission and reflection matrices are

$$\mathbf{t}(n+1,n)=\mathbf{G}^{+-}[\Delta^{+}\mathbf{A}+\mathbf{g}^{+-}\mathbf{g}^{-+}],$$

$$\mathbf{t}(n,n+1)=\mathbf{G}^{-+}[\Delta^{-}\mathbf{D}+\mathbf{g}^{-+}\mathbf{g}^{+-}],$$

$$\mathbf{r}(n+1,n)=\mathbf{G}^{-+}\mathbf{g}^{-+}[\mathbf{I}-\Delta^{+}\mathbf{A}],$$

$$\mathbf{r}(n,n+1)=\mathbf{G}^{+-}\mathbf{g}^{+-}[\mathbf{I}-\Delta^{-}\mathbf{D}].$$

The source vectors are

$$\mathbf{\Sigma}^{+}(n+1,n)=\mathbf{G}^{+-}[\Delta^{+}\mathbf{S}^{+}+\mathbf{g}^{+-}\Delta^{-}\mathbf{S}^{-}]\tau,$$

$$\mathbf{\Sigma}^{-}(n,n+1)=\mathbf{G}^{-+}[\Delta^{-}\mathbf{S}^{-}+\mathbf{g}^{-+}\Delta^{+}\mathbf{S}^{+}]\tau.$$